

Article

Coronatine Enhances Stalk Bending Resistance of Maize, Thickens the Cell Wall and decreases the Area of the Vascular Bundles

Yanxia Li, Guanmin Huang, Yuling Guo, Yuyi Zhou and Liusheng Duan *

College of Agronomy and Biotechnology, China Agricultural University, Beijing 100193, China; liyanxia@cau.edu.cn (Y.L.); bs20193010037@cau.edu.cn (G.H.); bs20193010036@cau.edu.cn (Y.G.); zhouyuyi@cau.edu.cn (Y.Z.)

* Correspondence: duanlsh@cau.edu.cn; Tel.: +86-010-62731301

Received: 20 April 2020; Accepted: 3 June 2020; Published: 5 June 2020



Abstract: Coronatine (COR) is a phytotoxin produced by the pathogen *Pseudomonas syringae*, it has a structure similar to that of jasmonates (JAs), but it is much more active as a plant growth regulator. The goal of this study was to gain more insight into the effect and the mechanism of COR effects on stalk characteristics are related lodging resistance of maize. The agronomic traits, stalk ultrastructure, and endogenous hormones in maize stalks were studied in field trails and greenhouses, using hybrid cultivar “Xianyu 335” (XY335), “Zhengdan 958” (ZD958) and inbred line B73 as materials in 2018 and 2019. Different concentration of COR were sprayed onto maize foliar surfaces at the seven-expanded-leaves (V_7) stage. Foliar application with $10 \mu\text{Mol L}^{-1}$ of COR at the V_7 stage decreased plant and ear height, increased weight and diameter of the basal internodes, and increased penetration strength and stalk bending resistance. Compared to the control treatment, in COR-treated plants, salicylic acid (SA) and jasmonic acid (JA) were decreased significantly in stalks. The treatment of $10 \mu\text{Mol L}^{-1}$ of COR enhanced lignin accumulation, the integrity, and the thickness of cell walls in maize stalks in the early stages of stem growth in the inbred line B73, as revealed by autofluorescence microscopy and scanning electron micrographs. Our results indicated that COR improved stalk bending resistance of maize not only by optimizing stalk morphological characteristics, but also by altering hormone levels, which may led to greater lignin accumulation, thickens cell wall, and decreased the area of vascular bundles.

Keywords: COR; maize; lodging resistance; cell wall; vascular bundle

1. Introduction

Maize (*Zea mays* L.) is one of the most important and highest yielding cereal crops in the world, with its annual yield representing approximately 34% of global cereal production [1] and 39% of total grain yield in China [2]. Though the strength of stalk has been improved in maize consistently, lodging is still one of the most important factors for the limitation maize yield to further increase. Lodging causes significant economic losses associated with reduced grain quality, grain yields, and harvesting efficiency. Approximately 5%–20% yield losses in the USA due to crop lodging [3], and a survey indicated that lodging reduces the annual maize yield in Japan by 15%–28% [4]. Sun et al. [5] reported that a 1% increase in lodging decreases maize production by an average of 108 kg ha^{-1} in China. The poor quality and grain yield caused by lodging have become unavoidable problems in crop production. Thus, one of the challenges of breeding and crop management is to enhance lodging resistance in maize. Breeders have developed and produced new varieties that are shorter and have stronger stalks through biotechnology and conventional breeding, and these have effectively improved the stalk-bending

resistance of maize and have decreased lodging risks [6]. In recent years, plant growth regulators have been able to modulate plant type, increase the lodging resistance [7] and increase grain yield [8,9] through the regulation of signaling and metabolite biosynthesis [10,11]. Many different kinds of plant growth regulators have been applied in crop production, such as ethephon [12], 3% diethyl aminoethyl hexanoate and 27% ethephon (EDTH) [8,9], chlornitequat chloride [13], and uniconazole [14].

Coronatine (COR) is not an endogenous phytohormone; it is a phytotoxin produced by several *Pseudomonas syringae* pathovars. The structure of COR is an amide of coronafacic acid and coronamic acid; it is a methyl cyclopropyl amino acid derived from isoleucine [15]. COR is a structural and functional analogue of jasmonates (JAs) [16,17] and related signaling compounds such as methyl jasmonic acid (MeJA) [18]. However, COR is highly active, approximately 10,000 folds more MeJA [19], and it is effective at extremely low concentrations—previous research has shown that 1 $\mu\text{Mol L}^{-1}$ of COR can improve resilience to abiotic stresses in plants [20]. Spraying 0.1 $\mu\text{Mol L}^{-1}$ of COR on a leaf could enhance drought tolerance in wheat by maintaining a high photosynthetic performance [21]. COR is a bacterial blight phytotoxin that can induce leaf chlorosis, increase ethylene generation, and accelerated senescence in infected crops [22–25]. Some research has suggested that COR is a plant growth regulator that plays a vital role for many crop growth processes in resistance to abiotic stress, such as drought and salinity stress, inducing anthocyanin production, the modulation of metabolism, hormone synthesis and transport, stomatal opening, and the elicitation of plant defenses [25–29]; 20 $\mu\text{Mol L}^{-1}$ of COR induced three-fold higher amounts of anthocyanin, and 2 $\mu\text{Mol L}^{-1}$ inhibited root growth in tomato seedlings [30]. COR is also involved in alkaloid accumulation, hypertrophy, tendril coiling, and leaf senescence [16,28,30]. There was a strong induction of the alkaloids in a concentration-dependent manner during COR treatment with various concentrations of COR (0.1–100 $\mu\text{Mol L}^{-1}$), and 100 $\mu\text{Mol L}^{-1}$ of COR increased the nicotine concentration of dry mass in tobacco [26]. Some researchers believe that COR has effect on the biosynthesis of chloroplasts [21].

Stalk strength is one of the most important agronomic properties of maize that is associated with grain yield [31]. The strength of a stalk is controlled by the morphological and compositional characteristics, such as plant height, ear height, stalk diameter, internode plumpness, and cell wall structural components such as lignin and cellulose [31–33]. The basal internodes of maize stalks play a vital role in lodging resistance [8,34]. The mechanical strength of maize stalks, such as rind penetration strength and dry weight per cm, is a good indicator of lodging resistance [35,36]. Thus, improving the basal internodes' physical strength is a new target of reducing the risk of crop lodging [8,35,37,38]. The maize stem is made up of various tissues and cell types, including vascular bundles, sclerenchyma, chlorenchyma, parenchyma, and the epidermis. Most of the small vascular bundles and sclerenchyma are located in the outer layer of the stalk. The pith is located in the inner part and mainly consists of a parenchyma with large vascular bundles. One of the primary factors that distinguishes plant stem tissues from one another are the thickness and localization of the cell walls of a given cell type or tissue. The main components of cell walls are pectins, cellulose, hemicellulose, protein, phenolics, and lignins. The differences of cell walls are closely related to their composition content.

Lignin is a main component of secondary cell walls, and it can thicken the cell wall and make it robust, thus improving mechanical strength to increase lodging resistance in crops [39,40]. A gradient distribution of bundle stiffness along the axial and radial directions of the stalk increases the strength of internodes, and it plays crucial roles in improving the lodging resistance of maize plants [41]. Fiber bundles are the main load-bearing structures of the stem and have highly lignified secondary cell walls. Fiber bundles are composed of numerous elementary fiber cells; the fiber cell can be divided into several laminate structures, and adjacent cells are bonded with each other by the middle laminate [42].

Previous research has shown that the application of plant growth regulators can improve lodging resistance in various crops. However, COR is a novel plant growth regulator, and little is known about the effects and the mechanism of COR on the mechanical strength and anatomical features of maize stalks. To address this lack of knowledge, we aimed to determine the effects of COR on stalk morphological characteristics, the ultrastructure of vascular bundles and cell walls, and their

relationship with stalk bending resistance in maize. The results of our research may provide guidance for the application of COR in agricultural production and some information regarding the development of cultural strategies that can improve lodging resistance and grain yield.

2. Materials and Methods

2.1. Experimental Site and Experimental Design

Field experiments were laid out to determine the stalk morphological characteristics of maize in 2018 and 2019 at the research station of Shandong Academy of Agricultural Sciences, Jinan, Shandong Province, China (36°58' N, 116°58' E). The experimental site was classified as semiarid with an average annual rainfall of 590 mm. The average content in the 0–20 cm tillage layer was 16.1 g kg⁻¹ of organic matter, 1.20 g kg⁻¹ of total nitrogen (N), 17.0 mg kg⁻¹ of rapidly available phosphorous (P), and 113 mg kg⁻¹ of rapidly available potassium contents (K). Field trials were carried out as a split plot design with three replicates in both planting seasons. The main plot treatments were cultivars, the sub-plot treatments were COR-treatments, and water foliar spray was used for controls that were randomly placed in the main plot. The area of the plot was 120 m² (6 m × 20 m). Hybrid maize cultivars Xianyu 335 (XY335—lodging-susceptible) and Zhengdan 958 (ZD958—lodging-resistant), which are widely planted in China, were used as experimental materials to research the effect of COR on agronomic traits and those related to the lodging resistance of maize. Maize was sown on June 5, 2018, and on June 1, 2019, at a density of 80,000 plants ha⁻¹ with 0.6 m row spacing. COR was applied to the foliar surfaces at concentrations of 1 μMol L⁻¹ (COR1), 10 μMol L⁻¹ (COR10), 30 μMol L⁻¹ (COR30), and 60 μMol L⁻¹ (COR60) with 0.01% (v/v) Tween 20 at the V₇ stage (when the 7th internode was 1 cm in length) in the afternoon (between 16:00 and 19:00). The COR solution was sprayed at a rate of 225 L ha⁻¹, and the same volume of water was applied to the control plants.

The gene sequence of Maize inbred line B73 is known. Plants were sown in plastic containers containing a mixture of commercial garden soil and vermiculite in a greenhouse at the China Agricultural University for the ultrastructural analysis and physiological assays. Under the 25/18 °C and 14/10 h day/night conditions. Deionized water (control, CK) and 10 μMol L⁻¹ of COR with 0.01% (v/v) Tween 20 were applied the leaves by using spray bottles at the V₇ stage. For each plant, 10 mL of solution was used, and each treatment had 20 plant replicates.

2.2. Sampling and Measurements

2.2.1. Morphological Trait and Bending Resistant Strength

Plant Height and Ear Height

Five maize plants in central rows were randomly cut at ground level at 20 days after the silking stage in each plot. Plant height was measured with a measuring tape from the base to the top of the tassel; ear height was measured to the first node bearing the ear.

Characteristics of the Third Basal Internode

We sprayed COR onto maize foliar surfaces at the V₇ stage, the seventh internode (the 3rd basal internode on the ground) began to elongate at this time because the internodes below the first four leaves never elongated, and the quality traits of the third to fifth basal internodes exhibited a significantly correlation with lodging resistance of maize, so the third basal internode was used to evaluate the quality of the stalks. Five maize plants in central rows were randomly collected to evaluate the characteristics of the third basal internode. We first removed the leaf blades and excised the third basal internode from the stem of each plant. The length of internode was measured with a ruler. The diameter was measured in the mid internode region by a digital caliper with an accuracy of 0.001 cm. The rind puncture strength was measured with a stalk strength tester (YYD-1, Zhejiang Top Instrument Co. Ltd., Hangzhou, China) by following the methods of Xu et al. [8]. To measure the dry

weight of the internodes, they were dried in an oven at 80 °C until they reached a constant weight. The dry weight per cm (g cm^{-1}) was calculated as the division of the dry weight (g) of the internode by the length (cm) of the internode. For fresh weight density, we measured the volume of the internode using the draining method. The specific operation was: we added a certain volume of water to a graduated cylinder and recorded the volume v_1 ; after that, we put the internode into the measuring cylinder with water and pressed the internode below the water surface with a glass rod, recording the volume of water and internode v_2 ; the volume of the internode $v = v_2 - v_1$. The fresh weight density was calculated by dividing the fresh weight of the internode by the volume of the internode.

2.2.2. Histological Analysis

Three maize plants were harvested from the CK and COR treatments at 5, 10, 15, and 20 days after spraying COR solution in the greenhouse. Sections were cut at the center of the 3rd basal internode from each stalk. Transverse and longitudinal sections were cut by hand with razor blades and then fixed for 24 h in a mixture of 2.5% glutaraldehyde and 2% paraformaldehyde in a 0.1% mol L^{-1} phosphoric acid buffer at 4 °C and post fixed in 1% osmium tetroxide on ice for 2 h and then washed with a fresh phosphate buffer saline (PBS) solution five times, each time for 20 min and then fixed using OsO_4 for 3 h. The samples were dehydrated in an ethanol series from 45% to 100% (30 min each time); afterwards, the samples were rinsed with isoamyl acetate twice (1 h each) and then vacuum dried. The dried samples were mounted on aluminum stubs, coated with gold using a sputter coater (SPI module, Structure Probe Inc., USA), and then viewed using a scanning electron microscope (S-3400N, SEM, Hitachi, Japan).

The middle of the 3rd basal internode was excised from the stem of each plant, fixed in Carnoy's solution (250 mL L^{-1} acetic acid with 750 mL L^{-1} ethanol), and then cross sections from the middle of the 3rd internode were cut by hand using razor blades. Lignin distribution was qualitatively evaluated by using autofluorescence microscopy. Lignin presents broad range of fluorescence emission and is excited with UV light [43]. Thus, lignified cell walls were quantified by autofluorescence microscopy [44]. To visualize lignin autofluorescence, tissue sections were visualized under UV excitation (360 to 390 nm) by a laser scanning microscope with airyscan (LSM 880, Zeiss, Germany). The fluorescence images were collected using a charge-coupled device (CCD) camera.

2.2.3. Phytohormone Quantification

Samples were collected at 5 days after the COR treatments. The leaves and the center of the 3rd basal internode samples were immediately frozen in liquid nitrogen and kept at -80 °C for COR, abscisic acid (ABA), auxin (IAA), jasmonic acid (JA), and salicylic acid (SA) quantification. In brief, three replicates of each frozen samples (100 mg) were ground in liquid nitrogen. We weighed 50 mg of powder into a 1.5 mL tube, an internal standard was added, samples were extracted in sequence, and extracts were centrifuged at 14,000 rpm for 5 min at 4 °C. Then, we extracted 1.2 mL of the lower organic phase that were dried in N_2 at room temperature, and then we resuspended the residue in 0.1 mL of MeOH. Then, the resuspended residue was filtered through a hydrophobic membranes using a nylon filter with a pore size of 0.22 μm .

The analytical conditions were as follows: Water Acquity ultra performance liquid chromatography-Class (Waters Corporation, 34 Maple Street Milford, MA, USA); column, Poroshell EC-120 (3.0 μm and 3.0 mm \times 100 mm); the mobile phase consisted of solvent A—pure water with 0.05% acetic acid—and solvent —acetonitrile with 0.05% acetic acid. Sample measurements were performed with a gradient program that employed the starting conditions of 10% A and 90% B. Within 10 min, a linear gradient to 10% A and 90% B was programmed, and a composition of 90% A and 10% B was kept for 0 min. The flow rate was held at 0.3 mL min^{-1} , 5 μL samples were injected, and then phytohormones were analyzed and quantified by a Q-Exactive high resolution mass spectrometer (Thermo Scientific, Waltham, MA, USA). The last step of LC-MS was carried out at the Biomass Bass Laboratory of China Agricultural University.

2.2.4. Measurement of Pushing Resistance

Lodging resistance was assessed using the measured of pushing resistance, which was carried out on the bottom part of the stalk following the method of Kashiwagi and Ishimaru [45]. At 20 days after the silking stage, the portable crop prostrate tester (AI-JGQD-01) was set perpendicularly at the basal internode of a maize stem about 50 cm above ground level, and the pushing resistance was measuring when plants were pushed to an angle from the vertical (Figure 1). The data collected by the hand-held equipment in the field when the system started to measure and the real-time curve of pressure and angle were plotted at the bottom of the interface.

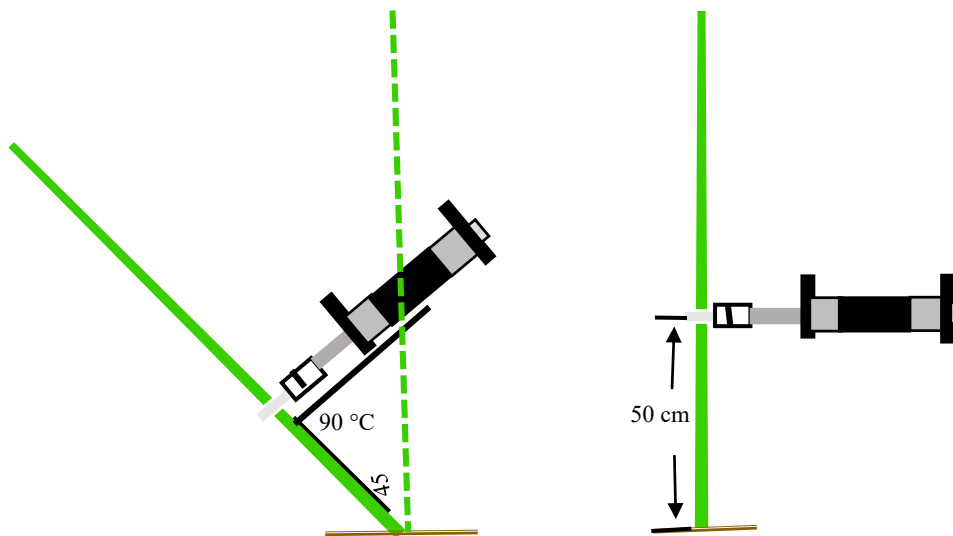


Figure 1. Schematic diagram of the measure method of pushing resistance.

2.3. Statistical Analyses

Data processing in all treatments was performed by Data Processing System software 9.50 (DPS) and Microsoft Excel 2003. Analyses of variance were judged by the least significant differences test using a 0.05 level of significance. Data plotting was performed with SigmaPlot 10.0. Pictures were quantitatively measured by ImageJ.

3. Results

3.1. Plant Height and Ear Height

Maize plant and ear heights responded to COR application in a manner dependent on dose in both cultivars in each year of growth. Shorter plant and ear heights were observed under COR treatments compared to the untreated control plants in the field trial. The plant height in COR1-, COR10-, COR30-, and COR60-treated ZD958 maize plants was reduced significantly by 3.0%, 9.8%, 42.5%, and 58.0%, respectively, in 2019, while reductions of 8.5%, 11.5%, 51.2%, and 29.5%, respectively, occurred in 2018. Upon COR1, COR10, COR30, and COR60 treatments, XY335 maize plant height was significantly reduced by 1.3%, 16.9%, 38.6%, and 40.2%, respectively, in 2019, while reductions of 1.7%, 9.1%, 28.2%, and 52.1%, respectively, were observed in 2018. Moreover, the ear height of ZD958 in COR1-, COR10-, COR30-, and COR60-treated plant heights was significantly reduced by 1.0%, 22.0%, 45.0%, and 49.0%, respectively, of that of control plants in 2019, and 12.5%, 27.1%, 48.2%, and 48.1% in 2018 respective to the increasing concentration series of COR treatment. The ear height of XY335 was significantly reduced by 26.7%, 29.0%, 36.3%, and 45.3% in 2019, respectively, and 4.9%, 22.5%, 39.2%, and 47.0% in 2018 over that of the control plants (Figure 2). Taken together, with higher concentrations of COR, plant and ear heights also decreased more severely. However, when the COR concentration was greater than or equal to $30 \mu\text{Mol L}^{-1}$ ($\geq 30 \mu\text{Mol L}^{-1}$), the growth of maize plants was poisoned, over-dwarfed the

plants, weak stem, and reduced biological yield, resulting in a smaller panicle or even no panicle of maize plants (Figure 2). The results indicated that COR had a concentration-dependent manner effect on maize plant during COR treatment with various concentrations.

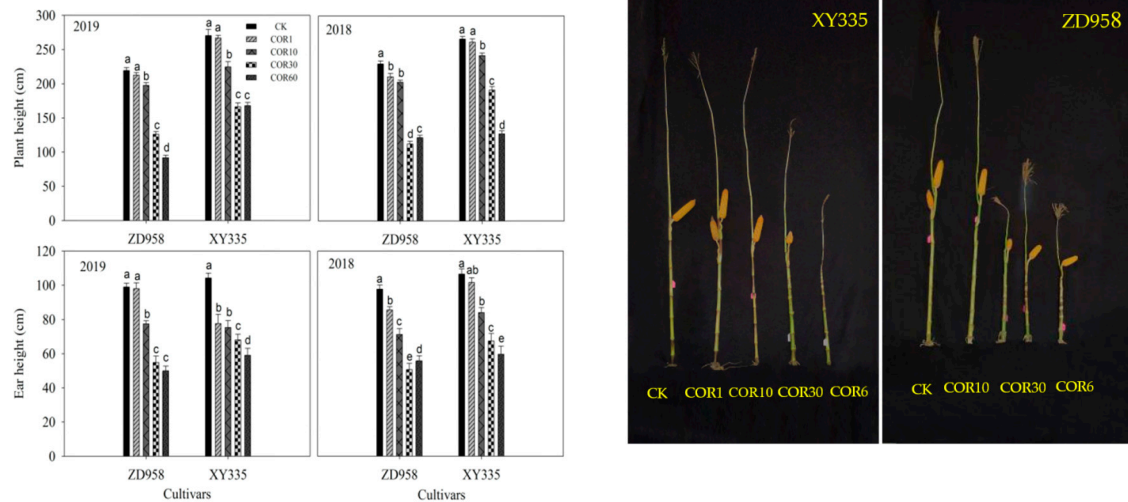


Figure 2. Effects of coronatine (COR) on maize plant height and ear height in field 2018 and 2019. ZD958: cultivar “Zhengdan958”; XY335: cultivar “Xanyu335”; CK: control treatment; COR1, COR10, COR30, and COR60 represent foliar application with coronatine at concentrations of 1, 10, 30, and 60 μM at the seventh-expanded-leaves stage, respectively.

3.2. Agronomic Traits of the 3rd Basal Internodes

To evaluate the alterations in the agronomic traits of maize stems in response to different concentrations of COR, the morphological characteristics and physical strength of the third basal internodes were assessed. The length of third basal internodes reduced with increasing concentrations of COR. Compared to the control treatment, COR1 had little effect on the length of the 3rd basal internode; COR10 reduced the internode length of ZD958 and XY335 by 19.5% and 10.0% in 2019 and 11.0% and 6.1% in 2018, respectively; COR30 substantially reduced the internode length of ZD958 and XY335 by 20.0% and 9.8% in 2019 and 36.4% and 5.2% in 2018, respectively; COR60 reduced the internode length of ZD958 and XY335 by 8.6% and 7.9% in 2019 and 0.1% and 6.3% in 2018, respectively. The degree of reduction of the third basal internode length with COR60 was similar to that with COR30. The average length of the third basal internodes for XY335 was higher than that of ZD958 by 53.6% and 31.4% in 2018 and 2019, respectively (Table 1).

The diameter of the third basal internodes was significantly increased with the COR10 treatment. Compared to the control treatment, the diameter of the third basal internode of ZD958 and XY335 with COR10 was greater by 12.3% and 10.1% in 2019 and 8.7%, and 3.7% in 2018, respectively (Table 1). However, the higher concentrations of COR ($\geq 30 \mu\text{Mol}^{-1}$) reduced the diameter of internodes, showing inhibitory effects.

The dry weight per cm of the third basal internodes exhibited an increasing pattern with increasing concentrations of COR in both years. The dry weight per cm of the third internode in COR1-, COR10-, COR30-, and COR60-treated ZD958 was higher by 4.2%, 5.6%, 7.0%, and 36.6% in 2019 and 11.0%, 12.3%, 5.5%, and 4.1% in 2018, respectively. For XY335, the dry weight per cm of the third internode was higher by 4.4%, 20.6%, 28.0%, and 30.9% in 2019 and 7.1%, 1.4%, 2.8%, and 25.7% in 2018 than that of control plants, respectively (Table 1). The highest tested concentration of COR (COR60) resulted in the greatest effect on the dry weight per cm of the third basal internodes among all the treatments except for ZD958 in 2018 (Table 1). Additionally, the trend of fresh weight density increased with increasing concentrations of COR (Table 1), with the fresh weight density of ZD958 being significantly higher than that of XY335 in cultivars.

Table 1. Effects of COR on the morphological characteristics and physical strength characteristics of the third basal internode in 2018 and 2019.

Years	Cultivers	Treatment	Length (cm)	Diameter (mm)	Volume (mL)	Cross Section Area (cm ²)	Fresh Weight (g)	Fresh Weight Density (g cm ⁻³)	Dry Weight (g)	Dry Weight per cm (g cm ⁻¹)	Ring Puncture Strength (Nmm ⁻²)	
2019	ZD958	Control	11.8 ± 0.8a	25.7 ± 0.3c	55.6 ± 1.2b	4.73 ± 0.5c	51.5 ± 1.3c	0.93 ± 0.03c	8.36 ± 0.5b	0.71 ± 0.04b	52.2 ± 4.2c	
		COR1	11.8 ± 1.0a	28.0 ± 0.5a	61.0 ± 2.8a	5.22 ± 0.8a	54.8 ± 2.5b	0.90 ± 0.04c	8.00 ± 0.7b	0.74 ± 0.02b	60.1 ± 3.8a	
		COR10	9.52 ± 0.9c	28.9 ± 0.2a	51.0 ± 1.3c	5.06 ± 0.4b	48.4 ± 3.0d	0.95 ± 0.06c	7.20 ± 0.4c	0.75 ± 0.05b	55.2 ± 5.5b	
		COR30	9.46 ± 0.7c	25.5 ± 0.6c	42.4 ± 0.9c	4.43 ± 0.3d	44.8 ± 1.9e	1.06 ± 0.04b	6.82 ± 0.6d	0.76 ± 0.07b	51.4 ± 4.6c	
		COR60	10.8 ± 1.2b	27.8 ± 1.2b	53.8 ± 1.5bc	5.03 ± 0.2b	58.0 ± 4.5a	1.08 ± 0.02a	10.5 ± 0.3a	0.97 ± 0.04a	50.5 ± 3.7c	
	XY335	Control	14.7 ± 0.5b	24.3 ± 0.4c	59.8 ± 2.4d	4.33 ± 0.7c	51.4 ± 2.8c	0.86 ± 0.06b	9.96 ± 0.6d	0.68 ± 0.02c	58.0 ± 2.6b	
		COR1	15.6 ± 0.7a	26.4 ± 0.6a	76.3 ± 1.5a	6.24 ± 0.3a	60.5 ± 3.2a	0.80 ± 0.07c	10.1 ± 0.7c	0.71 ± 0.01c	60.0 ± 6.2a	
		COR10	13.2 ± 0.6c	26.8 ± 1.2a	64.8 ± 2.0bc	4.89 ± 1.1b	57.1 ± 1.7b	0.89 ± 0.05b	10.8 ± 0.5c	0.82 ± 0.06b	61.7 ± 5.2a	
		COR30	13.2 ± 1.1c	25.1 ± 0.8b	65.8 ± 1.4b	4.97 ± 0.5b	57.8 ± 3.4b	0.87 ± 0.07b	11.7 ± 0.6b	0.89 ± 0.04a	58.0 ± 1.9b	
		COR60	13.5 ± 0.9c	24.9 ± 1.1bc	62.0 ± 2.8c	4.90 ± 0.8b	57.3 ± 4.1b	0.92 ± 0.06a	12.6 ± 0.9a	0.93 ± 0.06a	41.9 ± 6.4c	
	Source of variation		C	**	*	**	**	**	**	**	**	**
			T	**	**	**	**	**	**	**	**	**
			C×T	**	**	**	**	**	**	**	**	**
	2018	ZD958	Control	10.3 ± 0.6a	26.0 ± 1.2b	46.4 ± 4.2c	4.48 ± 0.3b	45.5 ± 2.7a	0.95 ± 0.02b	7.56 ± 0.5bc	0.73 ± 0.03b	45.4 ± 3.3b
COR1			10.6 ± 0.8a	26.4 ± 0.5b	48.8 ± 1.8a	4.68 ± 0.6b	45.0 ± 3.0d	0.92 ± 0.04b	8.63 ± 0.4a	0.81 ± 0.02a	46.9 ± 4.0a	
COR10			9.20 ± 1.0b	28.3 ± 0.8a	47.2 ± 0.9b	5.13 ± 0.4a	47.9 ± 1.8ab	1.01 ± 0.06a	7.56 ± 0.6bc	0.82 ± 0.05a	45.9 ± 1.9b	
COR30			6.58 ± 1.2c	25.5 ± 1.4c	34.8 ± 1.0d	5.16 ± 0.5c	29.5 ± 4.5e	0.85 ± 0.08c	6.46 ± 0.5c	0.97 ± 0.06b	40.3 ± 2.4c	
COR60			10.2 ± 0.7a	25.3 ± 0.6c	46.0 ± 1.7c	4.48 ± 0.8b	46.9 ± 1.6c	1.02 ± 0.06a	7.80 ± 0.7b	0.76 ± 0.08b	26.5 ± 6.3d	
XY335		Control	14.7 ± 0.8a	24.5 ± 0.9b	66.4 ± 2.9a	4.51 ± 0.3b	52.3 ± 2.6c	0.80 ± 0.04c	10.3 ± 0.5bc	0.70 ± 0.09c	55.4 ± 7.5b	
		COR1	14.6 ± 1.0a	23.5 ± 0.5c	63.4 ± 3.5b	4.32 ± 0.5d	50.5 ± 3.4d	0.81 ± 0.03b	10.7 ± 0.4b	0.75 ± 0.04b	59.7 ± 6.4a	
		COR10	13.8 ± 0.4a	25.4 ± 0.3a	63.8 ± 5.0b	4.61 ± 0.4a	53.8 ± 1.6b	0.84 ± 0.05b	10.1 ± 0.6c	0.73 ± 0.06c	56.2 ± 2.9b	
		COR30	13.9 ± 0.9b	24.2 ± 0.7bc	61.8 ± 3.0c	4.44 ± 0.6c	52.3 ± 2.4c	0.85 ± 0.04b	9.76 ± 0.3d	0.72 ± 0.04c	48.7 ± 4.2c	
		COR60	13.7 ± 0.6b	24.7 ± 0.6b	60.0 ± 1.4d	4.39 ± 0.5d	54.5 ± 3.3a	0.91 ± 0.06a	11.9 ± 0.2a	0.88 ± 0.05a	14.5 ± 3.1d	
Source of variation		C	**	*	**	**	**	**	**	**	**	
		T	**	**	**	*	**	**	**	**	**	
		C×T	**	**	**	*	**	**	**	**	**	

Different small letters within a column indicate significant differences across all treatments at $p < 0.05$ (least significant difference (LSD) test). COR1, COR10, COR30, and COR60 represent COR being sprayed onto maize foliar surfaces at the V₇ stage at concentrations of 1, 10, 30, and 60 $\mu\text{Mol L}^{-1}$. CK: control treatment; C: cultivars; T: treatments. * and ** indicate significance at the 0.05 and 0.01 probability levels, respectively.

The rind puncture strength of the third basal internodes was significantly affected by COR concentrations. Increasing COR concentration resulted in a rind puncture strength of the third internodes that first increased and then decreased. Compared to the control treatment, the rind puncture strength of the COR1 and COR10 treatments was higher, but the rind puncture strength of COR30 and COR60 was lower for both cultivars in each year. Rind puncture strength was ranked as COR10 > COR1 > CK > COR30 > COR60 in XY335 in 2019 and COR1 > COR10 > CK > COR30 > COR60 in XY335 in 2018 and ZD958 in both years.

3.3. Detection of Endogenous Hormone Contents

We detected the contents of the endogenous hormones in the stems and leaves of maize treated with COR. Our results (Figure 3) showed that compared to the control plants, COR was still present in leaves but was not detected in stems five days after $10 \mu\text{Mol L}^{-1}$ of COR solution was sprayed on maize foliar surfaces. These results indicated that there was a remnant of COR in the leaf, but there was no residual of COR in the stem at five days after COR application to the foliage surfaces. After COR treatment, the SA content increased and reached a significant level in the leaves, while the ABA and IAA contents decreased slightly at statistically insignificant levels. In the stem, SA and JA levels decreased significantly, while the IAA content decreased and ABA content increased to an insignificant level in the COR treatment group.

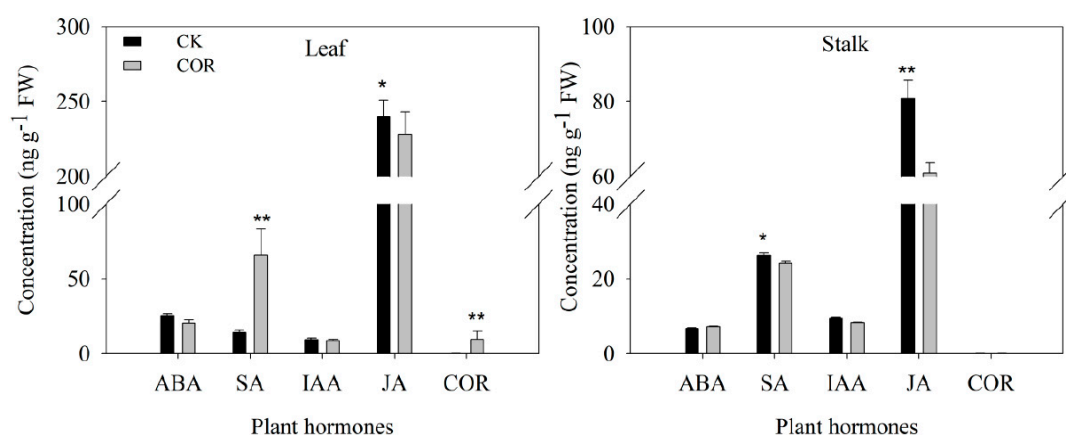


Figure 3. Effects of COR on endogenous hormone content in stalks and leaves of maize inbred line B73 plants in greenhouse. CK: control treatment; COR: $10 \mu\text{Mol L}^{-1}$ COR treatment; ABA: abscisic acid; SA: salicylic acid; IAA: auxin; JA: jasmonic acid; COR: coronatine. * and ** indicate significance at the 0.05 and 0.01 probability levels.

3.4. Microstructure Analysis of Maize Stalk

3.4.1. Lignin Distribution in Stalks Identified by Autofluorescence Microscopy

In our experimental study, lignin distribution and content in stem transverse sections were qualitatively measured by autofluorescence microscopy during stem development to investigate the lignin accumulation patterns in maize stems. The UV-excited fluorescence in the transverse sections of a maize inbred line B73 stem is shown in Figure 4. Lignin accumulation gradually increased in the stem tissues after $10 \mu\text{Mol L}^{-1}$ of COR treatment, with minimal lignification observed at five days and strong lignification observed at 20 days after COR treatment. Compared to the control treatment, a strong intensity of autofluorescence was detected in vascular bundles at an early stage (5–10 days) after treatments in the COR treatment group. Lignin was mainly deposited in the cell walls of vascular bundle sheaths, xylem, and sclerenchyma. The lignin fluorescence in CK plants increased as stem development progressed and was higher than that of the COR-treated plants at 15 days after treatment. Lignin fluorescence was found to be stronger in the CK stems at 20 days compared to

the COR treatment. Our results demonstrated that COR enhanced lignin accumulation at the early stages of stem development, but COR treatment was not conducive to the deposition of lignin in the later stage.

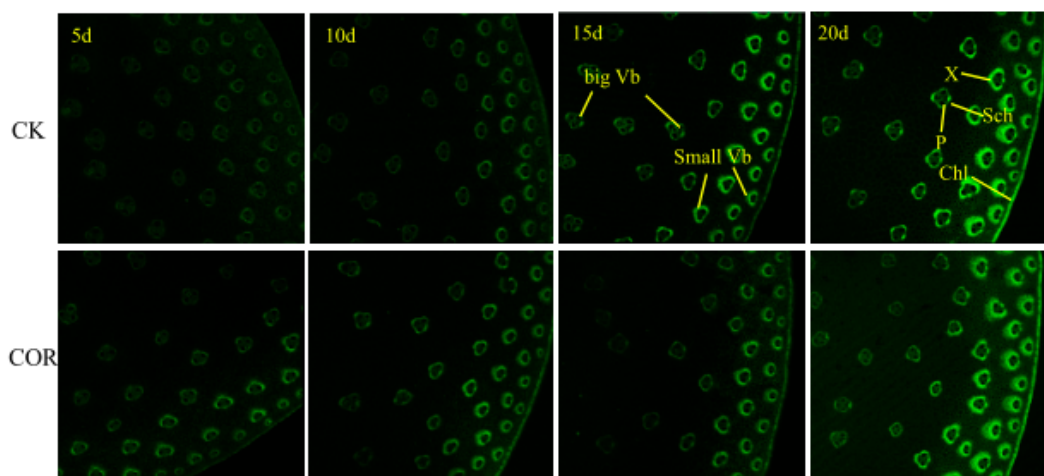


Figure 4. Fluorescence micrographs showing differences in the lignin composition in the walls of sclerenchyma cells and vascular bundles (sections were taken from the middle of the third internode) of maize inbred line B73 stems at different days after COR was sprayed onto foliar surfaces. CK: control treatment; COR10: $10 \mu\text{Mol L}^{-1}$ COR treatment. 5 d, 10 d, 15 d, and 20 d: respectively 5, 10, 15, and 20 days after COR treatment. Small vascular bundle (Vb): underdeveloped Vb, which are close to the edge of the stem; Big Vb: mature Vb, which are distributed in the central of the stem; P: phloem; X: xylem; Scl: sclerenchyma; Chl: chlorenchyma.

3.4.2. Scanning Electron Micrographs of Vascular Bundles and Cell Walls

Figure 5 shows scanning electron micrographs of the cross-section of vascular bundles. The vascular bundle consists of protoxylem vessels (PX), metaxylem vessels (MX), phloem tissue (Ph), and the vascular bundle sheath (VBS). Compared to the control treatment, the area of the vascular bundle cross-sectional gradually decreased in COR treatment, mainly due to VBS thickening and a gradual decrease in PX area (Table 2). In addition, compared to the COR treatment plants, in the CK group, the cell walls were thinner and there were many holes (a natural part of anatomy) in the cell wall at five days after the treatment (Figure 5). This suggests that COR treatment bolstered the integrity and the thickness of the cell wall at the early stages of stem development.

By using scanning electron microscopy, we also observed the cell walls of the maize stem in longitudinal sections and transverse sections at 15 days after COR treatment. Figure 6 shows the longitudinal section and the transverse section. Under $\times 350\text{X}$ magnification, we observed that the tension of the cell walls was relatively looser in COR treatment than that in CK treatment. Meanwhile, the cell walls in the CK treatment were tightly arranged.

3.5. Pushing Resistance of Maize Stalks

The real-time curve of pressure and angle is shown in Figure 7. The pressure stress increased when the tilt angle was pushed from the vertical. In both cultivars, COR10 treatment increased the pressure stress. The pressure stress was higher in ZD958 than that of in XY335 when plants were pushed to an angle from the vertical. Our results clearly indicated that the resistance to the bending of the stalk in ZD958 was higher than that of XY335, and COR10 could enhance the stalk bending resistance.

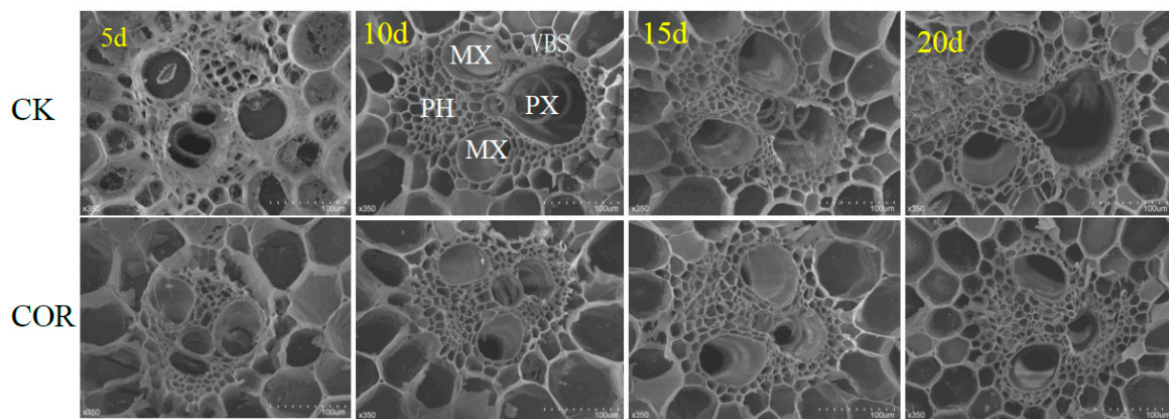


Figure 5. Scanning electron microscopy of the transverse sections of vascular bundles in the middle of the third basal internode at different numbers of days after COR was sprayed onto foliar surfaces in maize inbred line B73 plants. PX: protoxylem vessel; MX: metaxylem vessel; PH: phloem tissue; VBS: vascular bundle sheath; CK: control treatment; COR10: 10 $\mu\text{Mol L}^{-1}$ COR-treatment. 5 d, 10 d, 15 d, and 20 d: respectively 5, 10, 15, and 20 days after COR treatment.

Table 2. The effects of COR on the areas of the vascular bundles and protoxylem vessel in Figure 5.

Areas (μm^2)	Treatments	5d	10d	15d	20
Vascular bundle	CK	35,443.2 \pm 102.7	50,076.9 \pm 149.2	39,799.2 \pm 450.6	50,822.6 \pm 550.9
	C	28,436.4 \pm 203.5	30,795.6 \pm 198.4	38,761.9 \pm 342.6	38,754.2 \pm 489.2
Protoxylem vessel	CK	4012.6 \pm 198.4	10,346.5 \pm 368.6	71,41.6 \pm 185.4	13,479.9 \pm 358.2
	COR	2407.1 \pm 105.2	3867.4 \pm 282.4	6487.5 \pm 196.7	1885.4 \pm 102.3

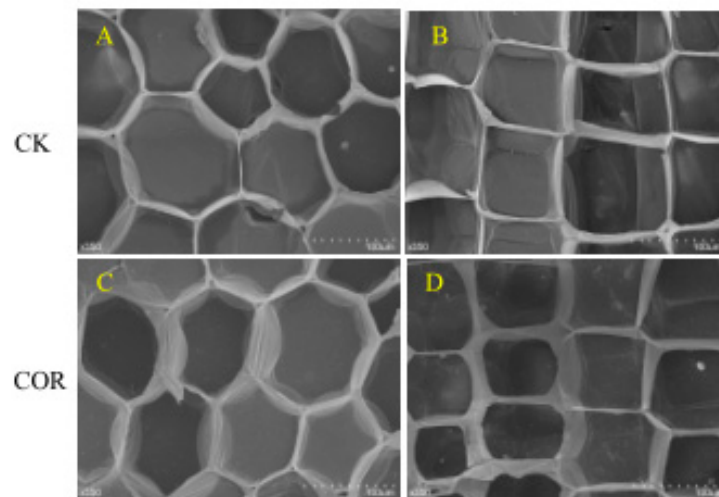


Figure 6. Scanning electron microscopy of the transverse and longitudinal structure of cells in the middle of the third basal internode of maize stalks at 15 days after COR was sprayed onto foliar surfaces. CK: control, COR10: 10 $\mu\text{Mol L}^{-1}$ COR treatment. (A) and (C) show transverse sections of the internode, and (B) and (D) show longitudinal sections of the inthenode.

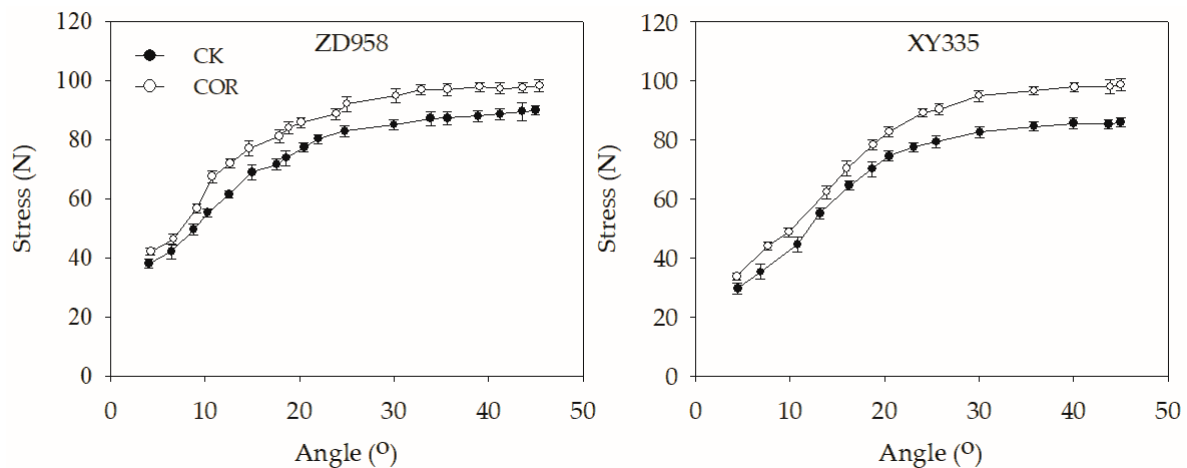


Figure 7. Effects of COR on the pushing resistance of the lower part in ZD958 and XY335 plants in 2018. ZD958: Cultivar “zhengdan958”; XY335: cultivar “Xanyu335”; CK: control treatment; COR10: $10 \mu\text{Mol L}^{-1}$ COR treatment.

4. Discussion

There are many factors that contribute to the lodging of maize, including plant morphology, plant density, stalk quality, root characteristics, genomic characteristics, damage caused by pests and diseases, water and fertilizers management, and environmental factors [46]. Enhancing the mechanical strength of stalks and controlling the morphological characteristics of plants are the major targets for increasing the lodging resistance of maize [6,38]. Previous research has shown that dry weight per cm and stem diameter are key indicators for evaluating lodging resistance in crops, as greater stem diameter and density and shorter basal internodes can enhance stalk bending resistance [47–49]. Reducing stem diameter, dry weight and lignin content in basal internodes in wheat and rice decrease lodging resistance [38,50]. In our study, our data indicated that spraying appropriate concentrations of COR onto maize foliar surfaces had significant effects on basal internodes and could enhance stalk lodging resistance. However, the higher concentration COR ($30 \mu\text{Mol L}^{-1}$) showed inhibitory effects on internode diameter, over-dwarfed the plants, and decreased the rind puncture strength, indicating that COR had a dosage-dependent effect on maize plant; this is in agreement with previous research [20,21]. Therefore, an appropriate COR concentration should be determined before using in the field. Based on our results, we suggest that COR should be applied at a concentration of $10 \mu\text{Mol L}^{-1}$ as a foliar application at the V_7 stage of maize to enhance stalk bending resistance.

The elastic modulus of the basal internodes is also strongly influenced by lodging resistance. It is a useful way to enhance the stalk bending of plants through increased the elastic modulus of fiber bundles in the basal internode by increasing the thickness of the cell wall and decreasing the area ratio of transverse sectional area occupied by phloem and vessels tissue [41]. Khanna [51] found that increasing the number of vascular bundles could enhance lodging resistance in wheat. However, other studies have reported that the vascular bundle number was not significantly related to the stalk strength in wheat [52] or barley [53]. Decreasing the diameter of vascular bundles could increase the stiffness of vascular bundles [54]. These conflicting results showed that the relationship between the anatomy characteristics of vascular bundles and stalk lodging resistance are still unclear. Considering the anatomy characteristics of vascular bundles, the two primary xylem vessels—MX and PX—are distinct in development and function. PX is differentiated first, and the spiral patterning of the secondary cell walls of PX allows for cell elongation; these cells are the dominant conductive elements for water in plants. In contrast, the secondary cell walls of MX are differentiated later in development and can be characterized by a rigid pitted pattern after the cessation of elongation growth [55]. In the present research, COR reduced the area of PX and the area of the vascular bundle (Figure 6). It can be inferred that such variations of the anatomy characteristics of vascular bundles influence the

spiral patterning and the secondary cell walls of PX, which could inhibit cell elongation, shorten the internode length of maize stalk, and be a vital factor of evaluating the lodging resistance in crop plants. The elastic modulus of vascular bundles may also be changed by fertilization strategies [37] or by using phytohormones [56]. Phytohormones have a vital role in plant cell elongation and cell wall biosynthesis and modification [57]. IAA leads to the inhibition of cell elongation [58] and has a negative effect on lignification [59]. SA mediates cell growth by controlling cell enlargement, endoreduplication, and cell division [60]. Application JA could freeze the cell mitosis, but the effect was sensitive to the phase of cell cycle [61]. Our results suggested that COR significantly decreased SA and JA in the stem, which may directly or indirectly regulate cell wall biosynthesis and manipulate the regulation of cell division, cell differentiation, and cell elongation. Together, these hormone-controlled processes contribute to changing the thicknesses of the cell wall and the area of vascular bundles, and they might be involved in affecting the diameter of internodes. Previous studies also have indicated that COR can thicken the cell wall of mesocotyl parenchyma [62]. It has been reported that phytohormones play important roles in the organization of the plant microtubule network [63], which is important for cell wall biosynthesis. However, the molecular mechanism of COR mediated the accumulation of lignin, and the synthesis of cell walls remains largely unclear and requires further investigation.

Plant growth depends on cell division and cell expansion/elongation. Maize internode elongation mainly depends on cell elongation and cell division. Our results suggest that COR could influence lignin accumulation and thicken cell walls in the early stage of internode elongation. A previous study indicated that cell walls play a crucial role in controlling the shape and size of a cell [64]. Cell wall synthesis, organization, and modification modulate cell volume and vacuolar turgor pressure, which have effects on plant cell growth [65]. The key requirement for cellular elongation is cell wall remodeling enzymes to loosen the cell wall by rearranging cell wall matrix polymers [65]. In our study, a higher level of lignin accumulation induced by COR-treated may have contributed to the lignification of cell walls (Figure 4). Increasing lignin deposition was found to thicken the cell walls, and plant tissues became stiffer. Similar results were demonstrated by Liu [63], who reported that COR could thicken cell walls. Lignin is mainly deposited in secondary cell walls, and it not only provides structural rigidity to the plant but also plays a vital role in mechanical support, nutrient and water transport, and plant pathogen defense [66]. Lignification thickens cell walls and could lead to the cessation of cell elongation or cell division in COR-treated internodes, thereby altering the chemical composition and anatomical features of the stem during the early stages of internode elongation and therefore changing agronomic traits and enhancing stalk bending resistance.

5. Conclusions

COR has a dose-dependent effect on the strength of maize stalks. Spraying an appropriate concentration of COR at the V₇ stage could increase the diameter, density, and rind penetration strength of basal internodes, thus improving stalk bending resistance. COR was found to alter hormone levels, manipulate cell wall biosynthesis and modification, decrease the area of protoxylem and vascular bundles, and increase the cell wall thickness, all of which may lead to the early cessation of cell division and cell elongation to reduce stem internode length and plant height.

Author Contributions: Conceptualization, methodology, investigation—Y.L., L.D.; field data collection and analysis—Y.L., Y.G.; resources, supervision—L.D.; writing and original draft preparation—Y.L., G.H., Y.Z.; funding acquisition—Y.L., L.D. All authors have read and agreed to the published version of the manuscript.

Funding: This study was financially supported by the National Natural Science Foundation of China (No.31801299) and the China Postdoctoral Science Foundation (No.2018M631632).

Conflicts of Interest: The authors declare that they have no conflicts of interest.

References

1. FAO. FAOSTAT-Agriculture Database. 2012. Available online: <http://faostat.fao.org/> (accessed on 5 May 2020).
2. National Bureau of Statistics of China. *Chinese Statistical Yearbook*; China Statistics: Beijing, China, 2014.
3. Norberg, O.S.; Mason, S.C.; Lowry, S.R. Ethephon influence on harvestable yield, grain quality, and lodging of corn. *Agron. J.* **1988**, *80*, 768–772. [[CrossRef](#)]
4. Minami, M.; Ujihara, A. Effects of lodging on dry matter production, grain yield and nutritional composition at different growth stages in maize (*Zea mays* L.). *Jpn. J. Crop Sci.* **1991**, *60*, 107–115. [[CrossRef](#)]
5. Sun, S.; Gu, W.; Dai, J. The effect of density on lodging of crop. *J. Shenyang Agric. Univ.* **1989**, *4*, 413–416.
6. Ma, D.L.; Xie, R.Z.; Liu, X.; Niu, X.K.; Hou, P.; Wang, K.R.; Lu, Y.L.; Li, S.K. Lodging-related stalk characteristics of maize varieties in china since the 1950. *Crop Sci.* **2014**, *54*, 2805–2814. [[CrossRef](#)]
7. Schluttenhofer, C.M.; Massa, G.D.; Mitchell, C.A. Use of uniconazole to control plant height for an industrial/pharmaceutical maize platform. *Ind. Crop. Prod.* **2011**, *33*, 720–726. [[CrossRef](#)]
8. Xu, C.L.; Gao, Y.B.; Tian, B.J.; Ren, J.H.; Meng, Q.F.; Wang, P. Effects of EDAH, a novel plant growth regulator, on mechanical strength, stalk vascular bundles and grain yield of summer maize at high densities. *Field Crops Res.* **2017**, *200*, 71–79. [[CrossRef](#)]
9. Zhang, Q.; Zhang, L.; Evers, J.; van der Werf, W.; Zhang, W.; Duan, L. Maize yield and quality in response to plant density and application of a novel plant growth regulator. *Field Crops Res.* **2014**, *164*, 82–89. [[CrossRef](#)]
10. Zeng, Q.; Jiang, L.; Wang, D.; Huang, S.; Yang, D. Camptothecin and 10-hydroxycamptothecin accumulation in tender leaves of *Camptotheca acuminata* saplings after treatment with plant growth regulators. *Plant Growth Regul.* **2012**, *68*, 467–473. [[CrossRef](#)]
11. Naeem, M.; Khan, M.M.A.; Moinuddin. Triacantanol: A potent plant growth regulator in agriculture. *J. Plant Interact.* **2012**, *7*, 129–142. [[CrossRef](#)]
12. Tripathi, S.C.; Sayre, K.D.; Kaul, J.N.; Narang, R.S. Growth and morphology of spring wheat (*Triticum aestivum* L.) culms and their association with lodging: Effects of genotypes, N levels and ethephon. *Field Crop. Res.* **2003**, *84*, 271–290. [[CrossRef](#)]
13. Ramburan, S.; Greenfield, P.L. Use of ethephon and chlormequat chloride to manage plant height and lodging of irrigated barley (cv. Puma) when high rates of N-fertiliser are applied. *S. Afr. J. Plant Soil.* **2007**, *24*, 181–187. [[CrossRef](#)]
14. Ahmad, I.; Kamran, M.; Ali, S.; Bilegjargal, B.; Cai, T.; Ahmad, S.; Meng, X.P.; Su, W.N.; Liu, T.N.; Han, Q.F. Uniconazole application strategies to improve lignin biosynthesis, lodging resistance and production of maize in semiarid regions. *Field Crop. Res.* **2018**, *222*, 66–77. [[CrossRef](#)]
15. Ichihara, A.; Shiraiishi, K.; Sato, H.; Sakamura, S.; Nishiyama, K.; Sakai, R.; Furusaki, A.; Matsumoto, T. The structure of coronatine. *J. Am. Chem. Soc.* **1977**, *99*, 636–637. [[CrossRef](#)]
16. Feys, B.J.F.; Benedetti, C.E.; Penfold, C.N.; Turner, J.G. Arabidopsis mutants selected for resistance to the phytotoxin coronatine are male sterile, insensitive to methyl jasmonate, and resistant to a bacterial pathogen. *Plant Cell.* **1994**, *6*, 751–759. [[CrossRef](#)] [[PubMed](#)]
17. Staswick, P.E.; Tiryaki, I. The oxylipin signal jasmonic acid is activated by an enzyme that conjugates it to isoleucine in Arabidopsis. *Plant Cell.* **2004**, *16*, 2117–2127. [[CrossRef](#)] [[PubMed](#)]
18. Dittrich, H.; Kutchan, T.M.; Zenk, M.H. The jasmonate precursor, 12-oxo-phytodienoic acid, induces phytoalexin synthesis in *Petroselinum crispum* cell cultures. *FEBS Lett.* **1992**, *309*, 33–36. [[CrossRef](#)]
19. Yan, J.B.; Zhang, C.; Gu, M.; Bai, Z.Y.; Zhang, W.G.; Qi, T.C.; Cheng, Z.W.; Peng, W.; Luo, H.B.; Nan, F.J.; et al. The arabidopsis CORONATINE INSENSITIVE1 protein is a jasmonate receptor. *Plant Cell.* **2009**, *21*, 2220–2236. [[CrossRef](#)] [[PubMed](#)]
20. Xie, Z.X.; Duan, L.S.; Li, Z.H.; Wang, X.D.; Liu, X.J. Dose-dependent effects of coronatine on cotton seedling growth under salt stress. *J. Plant Growth Regul.* **2015**, *34*, 651–664. [[CrossRef](#)]
21. Zhou, Y.Y.; Liu, Y.R.; Peng, C.X.; Li, X.W.; Zhang, M.C.; Tian, X.L.; Li, J.M.; Li, Z.H.; Duan, L.S. Coronatine enhances drought tolerance in winter wheat by maintaining high photosynthetic performance. *J. Plant Physiol.* **2018**, *228*, 59–65. [[CrossRef](#)]
22. Bender, C.L.; Alarcon, C.F.; Gross, D.C. Pseudomonas syringae phytotoxins: Mode of action, regulation and biosynthesis by peptide and polypeptide synthetases. *Microbiol. Mol. Biol. Rev.* **1999**, *63*, 266–292. [[CrossRef](#)]
23. Melotto, M.; Underwood, W.; He, S.Y. Role of stomata in plant innate immunity and foliar bacterial disease. *Ann. Rev. Phytopathol.* **2008**, *46*, 101–122. [[CrossRef](#)]

24. Kenyon, J.S.; Turner, J.G. Physiological changes in nicotiana tabacum leaves during development of chlorosis caused by coronatine. *Physiol. Mol. Plant Pathol.* **1990**, *37*, 463–477. [[CrossRef](#)]
25. Kenyon, J.S.; Turner, J.G. The stimulation of ethylene synthesis in nicotiana tabacum leaves by the phytotoxin coronatine. *Plant Physiol.* **1992**, *100*, 219–224. [[CrossRef](#)] [[PubMed](#)]
26. Schüler, G.; Mithöfer, A.; Baldwin, I.T.; Berger, S.; Ebel, J.; Santos, J.G.; Herrmann, G.; Hölscher, D.; Kramell, R.; Kutchan, T.M.; et al. Coronalon: A powerful, tool in plant stress physiology. *EFBS Lett.* **2004**, *563*, 17–22. [[CrossRef](#)]
27. Xie, Z.X.; Duan, L.S.; Tian, X.L.; Wang, B.M.; Eneji, A.E.; Li, Z.H. Coronatine alleviates salinity stress in cotton by improving the antioxidative defense system and radical-scavenging activity. *J. Plant Physiol.* **2008**, *165*, 375–384. [[CrossRef](#)]
28. Zhang, Z.Y.; Yang, F.Q.; Li, B.; Eneji, A.E.; Li, J.M.; Duan, L.S.; Wang, B.M.; Li, Z.H.; Tian, X.L. Coronatine-induced lateral-root formation in cotton (*Gossypium hirsutum*) seedlings under potassium-sufficient and deficient conditions in relation to auxin. *J. Plant Nutr. Soil Sci.* **2009**, *172*, 435–444. [[CrossRef](#)]
29. Geng, X.Q.; Jin, L.; Shimada, M.; Kim, M.G.; Mackey, D. The phytotoxin coronatine is a multifunctional component of the virulence armament of *Pseudomonas syringae*. *Planta* **2014**, *240*, 1149–1165. [[CrossRef](#)]
30. Uppalapati, S.R.; Ayoubi, P.; Weng, H.; Palmer, D.A.; Mitchell, R.E.; Jones, W.; Bender, C.L. The phytotoxin coronatine and methyl jasmonate impact multiple phytohormone pathways in tomato. *Plant J.* **2005**, *42*, 201–217. [[CrossRef](#)]
31. Peiffer, J.A.; Flint-Garcia, S.A.; Leon, N.D.; McMullen, M.D.; Kaeppeler, S.M.; Buckler, E.S. The genetic architecture of maize stalk strength. *PLoS ONE* **2013**, *8*, e67066. [[CrossRef](#)]
32. Baker, C.J.; Sterling, M.; Berry, P. A generalised model of crop lodging. *J. Theor. Biol.* **2014**, *363*, 1–12. [[CrossRef](#)]
33. Bosch, M.; Mayer, C.D.; Cookson, A.; Donnison, I.S. Identification of genes involved in cell wall biogenesis in grasses by differential gene expression profiling of elongating and non-elongating maize internodes. *J. Exp. Bot.* **2011**, *62*, 3545–3561. [[CrossRef](#)] [[PubMed](#)]
34. Zhang, J.; Li, G.H.; Song, Y.P.; Liu, Z.H.; Yang, C.D.; Tang, S.; Zheng, C.Y.; Wang, S.H.; Ding, Y.F. Lodging resistance characteristics of high-yielding rice populations. *Field Crops Res.* **2014**, *161*, 64–74. [[CrossRef](#)]
35. Flint-Garcia, S.A.; Jangpatong, C.; Darrach, L.L.; McMullen, M.D. Quantitative trait locus analysis of stalk strength in four maize populations. *Crop Sci.* **2003**, *43*, 13–22. [[CrossRef](#)]
36. Gou, L.; Huang, J.J.; Sun, R.; Ding, Z.S.; Dong, Z.Q.; Zhao, M. Variation characteristic of stalk penetration strength of maize with different density tolerance varieties. *Trans. CSAE* **2010**, *26*, 156–162. [[CrossRef](#)]
37. Wang, C.; Ruan, R.W.; Yuan, X.H.; Hu, D.; Yang, H.; Li, Y.; Yi, Z.L. Effects of nitrogen fertilizer and planting density on the lignin synthesis in the culm in relation to lodging resistance of buckwheat. *Plant Prod. Sci.* **2015**, *18*, 218–227. [[CrossRef](#)]
38. Zheng, M.J.; Chen, J.; Shi, Y.H.; Li, Y.X.; Yin, Y.P.; Yang, D.Q.; Luo, Y.L.; Pang, D.W.; Xu, X.; Li, W.Q.; et al. Manipulation of lignin metabolism by plant densities and its relationship with lodging resistance in wheat. *Sci. Rep.* **2017**, *7*, 41805. [[CrossRef](#)]
39. Peng, D.L.; Chen, X.G.; Yin, Y.P.; Lu, K.L.; Yang, W.B.; Tang, Y.H.; Wang, Z.L. Lodging resistance of winter wheat (*Triticum aestivum* L.): Lignin accumulation and its related enzymes activities due to the application of paclobutrazol or gibberellin acid. *Field Crops Res.* **2014**, *157*, 1–7. [[CrossRef](#)]
40. Chen, X.G.; Shi, C.Y.; Yin, Y.P.; Wang, Z.L.; Shi, Y.H.; Peng, D.L.; Ni, Y.L.; Cai, T. Relationship between lignin metabolism and lodging resistance in wheat. *Acta Agron. Sin.* **2011**, *37*, 1616–1622. [[CrossRef](#)]
41. Huang, J.L.; Liu, W.Y.; Zhou, F.; Peng, Y.J.; Wang, N.L. Mechanical properties of maize fibre bundles and their contribution to lodging resistance. *Biosyst. Eng.* **2016**, *151*, 298–307. [[CrossRef](#)]
42. Wang, N.L.; Liu, W.Y.; Peng, Y. Gradual transition zone between cell wall layers and its influence on wood elastic modulus. *J. Mater. Sci.* **2013**, *48*, 5071–5084. [[CrossRef](#)]
43. Donaldson, L.A.; Knox, J.P. Localization of cell wall polysaccharides in normal and compression wood of radiata pine: Relationships with lignification and microfibril orientation. *Plant Physiol.* **2012**, *158*, 642–653. [[CrossRef](#)] [[PubMed](#)]
44. Saito, K.; Fukushima, K. Distribution of lignin interunit bonds in the differentiating xylem of compression and normal woods of *Pinus thunbergii*. *J. Wood Sci.* **2005**, *51*, 246–251. [[CrossRef](#)]

45. Kashiwagi, T.; Ishimaru, K. Identification and functional analysis of a locus for improvement of lodging resistance in rice. *Plant Physiol.* **2004**, *134*, 676–683. [[CrossRef](#)] [[PubMed](#)]
46. Xue, J.; Xie, R.Z.; Zhang, W.F.; Wang, K.R.; Hou, P.; Ming, B.; Gou, L.; Li, S.K. Research progress on reduced lodging of high-yield and -density maize. *J. Integr. Agric.* **2017**, *16*, 2717–2725. [[CrossRef](#)]
47. Kokubo, A.; Kuraishi, S.; Sakurai, N. Culm strength of barley, correlation among maximum bending stress, cell wall dimensions, and cellulose content. *Plant Physiol.* **1989**, *91*, 876–882. [[CrossRef](#)]
48. Zhong, R.Q.; Taylor, J.J.; Ye, Z.H. Disruption of interfascicular fiber differentiation in a Arabidopsis mutant. *Plant Cell.* **1997**, *9*, 2159–2170. [[CrossRef](#)]
49. Kaack, K.; Schwarz, K.U.; Brander, P.E. Variation in morphology, anatomy and chemistry of stems of Miscanthus genotypes differing in mechanical properties. *Ind. Crops Prod.* **2003**, *17*, 131–142. [[CrossRef](#)]
50. Weng, F.; Zhang, W.; Wu, X.; Xu, X.; Ding, Y.; Li, G.; Liu, Z.; Wang, S. Impact of low-temperature, overcast and rainy weather during the reproductive growth stage on lodging resistance of rice. *Sci. Rep.* **2017**, *7*, 1–9. [[CrossRef](#)]
51. Khanna, V.K. Relationship of lodging resistance and yield to anatomical characters of stem in wheat, triticale and rye. *Wheat Inf. Serv.* **1991**, *73*, 19–24.
52. Zuber, U.; Winzeler, H.; Messmer, M.M.; Keller, M.; Keller, B.; Schmid, J.E.; Stamp, P. Morphological traits associated with lodging resistance of spring wheat (*Triticum aestivum* L.). *J. Agron. Crop Sci.* **1999**, *182*, 17–24. [[CrossRef](#)]
53. Dunn, G.; Briggs, K.G. Variation in culm anatomy among barley cultivars differing in lodging resistance. *Can. J. Bot.* **1989**, *67*, 1838–1843. [[CrossRef](#)]
54. Mwaikambo, L.Y. Tensile properties of alkalisized jute fibres. *Bioresource* **2009**, *4*, 566–588.
55. Esau, K. *Anatomy of Seed Plants*, 2nd ed.; Wiley: New York, NY, USA, 1977.
56. Okuno, A.; Hirano, K.; Asano, K.; Takase, W.; Masuda, R.; Morinaka, Y.; Ueguchi-Tanaka, M.; Kitano, H.; Matsuoka, M. New approach to increasing rice lodging resistance and biomass yield through the use of high gibberellin producing varieties. *PLoS ONE* **2014**, *9*, e86870. [[CrossRef](#)] [[PubMed](#)]
57. Didi, V.; Jackson, P.; Hejatko, J. Hormonal regulation of secondary cell wall formation. *J. Exp. Bot.* **2015**, *66*, 5015–5027. [[CrossRef](#)]
58. Lin, D.S.; Cao, L.Y.; Zhou, Z.Z.; Zhu, L.; Ehrhardt, D.; Yang, Z.B.; Fu, Y. Rho GTPase signaling activates microtubule severing to promote microtubule ordering in Arabidopsis. *Curr. Biol.* **2013**, *23*, 290–297. [[CrossRef](#)]
59. Cecchetti, V.; Altamura, M.M.; Brunetti, P.; Petrocelli, V.; Falasca, G.; Ljung, K.; Costantino, P.; Cardarelli, M. Auxin controls Arabidopsis anther dehiscence by regulating endothecium lignification and jasmonic acid biosynthesis. *Plant J.* **2013**, *74*, 411–422. [[CrossRef](#)]
60. Vanacker, H.; Lu, H.; Rate, D.N.; Greenberg, J.T. A role for salicylic acid and NPR1 in regulating cell growth in Arabidopsis. *Plant J.* **2001**, *28*, 209–216. [[CrossRef](#)]
61. Swiatek, A.; Lenjou, M.; Van, B.D.; Dirk, I.; Harry, V.O. Differential Effect of Jasmonic Acid and Abscisic Acid on Cell Cycle Progression in Tobacco BY-2 Cells. *Plant Physiol.* **2002**, *128*, 201–211. [[CrossRef](#)]
62. Liu, Y.R.; Zhou, Y.Y.; Huang, G.M.; Zhu, N.N.; Li, Z.H.; Zhang, M.C.; Duan, L.S. Coronatine inhibits mesocotyl elongation by promoting ethylene production in etiolated maize seedlings. *Plant Growth Regul.* **2019**, *90*, 51–61. [[CrossRef](#)]
63. Shibaoka, H. Plant hormone-induced changes in the orientation of cortical microtubules- alterations in the cross-linking between microtubules and the plasma-membrane. *Annu. Rev. Plant Physiol. Plant Mol. Bio.* **1994**, *45*, 527–544. [[CrossRef](#)]
64. Kalve, S.; Fotschki, J.; Beeckman, T.; Vissenberg, K.; Beemster, G.T.S. Three-dimensional patterns of cell division and expansion throughout the development of Arabidopsis thaliana leaves. *J. Exp. Bot.* **2014**, *65*, 6385–6397. [[CrossRef](#)] [[PubMed](#)]
65. Cosgrove, D.J. Expansive growth of plant cell walls. *Plant Physiol. Biochem.* **2000**, *38*, 109–124. [[CrossRef](#)]
66. You, T.T.; Mao, J.Z.; Yuan, T.Q.; Wen, J.L.; Xu, F. Structural elucidation of the lignins from stems and foliage of arundo donax Linn. *J. Agric. Food Chem.* **2013**, *61*, 5361–5370. [[CrossRef](#)] [[PubMed](#)]

